

Fabrication and characterization of polymer composites surface coated Fe₃O₄/MWCNTs hybrid buckypaper as a novel microwave-absorbing structure

Shaowei Lu, Keming Ma, Xiaoqiang Wang, Xuhai Xiong, Weikai Xu, Caixia Jia

Faculty of Aerospace Engineering, Shenyang Aerospace University, Shenyang 110136, China

Correspondence to: S.-W. Lu (E-mail: lushaowei_2005@163.com)

ABSTRACT: A naval hybrid buckypaper was fabricated by vacuum filtration method with monodispersion solution of Fe₃O₄ decorated Multiwalled carbon nanotubes (MWCNTs). The morphology, element composition and phase structure of hybrid buckypaper were characterized by field-emission scanning electron microscope, energy dispersive spectrometer, and X-ray diffraction. The microwave absorption and complex electromagnetic properties of the composites surface coated MWCNTs buckypaper (or Fe₃O₄/MWCNTs hybrid buckypaper) have been investigated in the frequency range of 8–18 GHz. The results indicate that the microwave absorption properties of composite structure have been evidently improved due to the Fe₃O₄/MWCNTs hybrid buckypaper' high magnetic loss and suitable dielectric loss properties. The reflection loss of composite surface coated Fe₃O₄/MWCNTs hybrid buckypaper (with a matching thickness $d = 0.1$ mm) is below -10 dB in the frequency range of 13–18 GHz, and the minimum value is -15.3 dB at 15.7 GHz. Thus, Fe₃O₄/MWCNTs hybrid buckypaper can become a promising candidate for electromagnetic-wave-absorption materials with strong-absorption, thin-thickness and light-weight characteristics. © 2015 Wiley Periodicals, Inc. *J. Appl. Polym. Sci.* **2015**, *132*, 41974.

KEYWORDS: adsorption; dielectric properties; films; magnetism and magnetic properties; non-polymeric materials and composites

Received 22 April 2014; accepted 12 January 2015

DOI: 10.1002/app.41974

INTRODUCTION

Since discovered by Iijima in 1991,¹ Carbon nanotubes (CNTs) have attracted much attention for their unique structure and intriguing properties. Due to their high aspect ratio, one-dimensional nanostructure and quantum effects, CNTs exhibit a good prospect application, especially in microwave-absorbing materials.

However, excellent microwave absorption properties cannot be obtained for unmodified CNTs because their magnetic loss is too small.² It is necessary to modify CNTs by decorating other nanomaterials, which are expected to exhibit ideal electromagnetic absorption properties.^{3,4} Surface functionalization of the CNTs and subsequent assembly of CNTs with preformed iron oxide nanoparticles via either covalent or non-covalent bonding is the common synthesis route. There are many methods for the preparation of Fe₃O₄/multiwalled carbon nanotubes (MWCNTs) hybrids,^{5–8} but the *in situ* chemical precipitation method is the mostly promising method.⁹

Traditionally, researcher fabricated composites by directly mixing the CNTs into polymers and made the final composites. However, CNTs' low solubility in common solvents, strong agglomerating tendency and high viscosity of polymer/CNTs mixtures caused a

poor dispersion. Besides the dispersion issue, the rapidly increasing viscosity of the mixture made high CNT loading nanocomposite fabrication to be difficult. To address these problems, CNTs sheets, also known as “buckypaper” have been recently used for the development of reinforcing composites. CNTs buckypaper are free-standing porous mats of entangled CNT ropes cohesively bounded by van der Waals interactions,^{10–12} commonly prepared by vacuum filtration through a membrane of a suspended solution of randomly distributed.¹³ Buckypaper is an ideal microwave absorption candidate due to the lightweight, exceptional high mechanical property and high conductivity of the CNTs.

In this article, we fabricated Fe₃O₄/MWCNTs hybrid buckypaper with monodisperse solutions of MWCNTs and Fe₃O₄ nanoparticles through vacuum filtration method. The electromagnetic and microwave absorption characteristics of the composites surface coated Fe₃O₄/MWCNTs hybrid buckypaper are investigated in the frequency range of 8–18 GHz.

EXPERIMENTAL

Materials

MWCNTs (ID: 10–30 nm, length: 50 μ m, purity: 98%) were provided by Chengdu organic chemicals., China Academy. Other

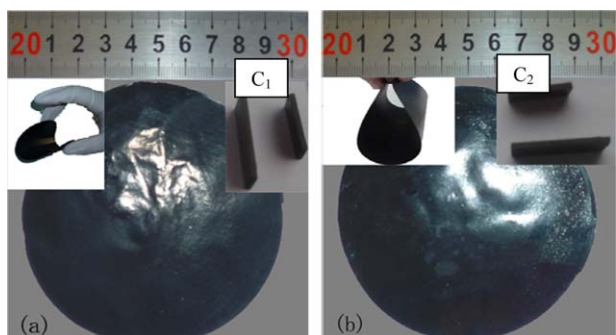


Figure 1. Buckypapers and composites surface coated buckypaper, (a) pure MWCNTs buckypaper, (b) hybrid MWCNTs buckypaper. [Color figure can be viewed in the online issue, which is available at wileyonlinelibrary.com.]

chemical reagents were all analytical grade and used without further purification. The glass fiber (GF) with a surface density of 200 g/m^2 was supplied by Composite One. A commercially available bisphenol A-type epoxy resin (618 type, Tianjin resin company) and an amine-type hardener [$\text{C}_{17}\text{H}_{31}\text{CONH}(\text{C}_2\text{H}_4\text{NH}_2)_2$] (Tianjin Ningping Chemical) were used to prepare the composite. The resin/curing agent ratio was 2 : 1.

Processing of Hybrid Nanopapers and Polymer Composite

The $\text{Fe}_3\text{O}_4/\text{MWCNTs}$ hybrid particles were fabricated by an *in situ* chemical precipitation method.⁹ MWCNTs (0.4146 g) and polyvinylpyrrolidone (PVP) (1 g) were first dissolved in 100 mL distilled water, the mixture solution was placed in an ultrasonic bath (99 w, 40 kHz) for 1 h, then $\text{FeCl}_3 \cdot 6\text{H}_2\text{O}$ (0.4206 g) and $\text{FeCl}_2 \cdot 4\text{H}_2\text{O}$ (0.1776 g) were added to this solution. After 25 min, 25 mL of $\text{NH}_3 \cdot \text{H}_2\text{O}$ (25%) was added drop wise to precipitate the iron oxides while the mixture solution was sonicating. The pH of the final mixture was in the range of 11–12. The reaction was carried out at 30°C for 60 min with constant mechanical stirring. The precipitates were collected with the aid of a magnet and washed to neutral with distilled water, and dried at 50°C for 48 h in a vacuum oven.

The pure-MWCNTs (or the $\text{Fe}_3\text{O}_4/\text{MWCNTs}$ hybrids) were first dispersed into water with the aid of TritonX-100 [$\text{C}_{14}\text{H}_{22}\text{O}(\text{C}_2\text{H}_4\text{O})$], the suspension was sonicating for 30 min with a high-intensity (Masonic sonicator 4000, Qsonica, LLC, Newtown, Connecticut, USA) at room temperature. The suspension was then filtrated through a $0.45 \mu\text{m}$ hydrophilic polycarbonate membrane under a negative pressure of 100 psi to separate the pure-MWCNTs (or the $\text{Fe}_3\text{O}_4/\text{MWCNTs}$ hybrids) from the solvent and form a nanopaper. After the filtration process, the nanopaper was dried in a heating oven at 80°C for 3 h to further remove the remaining water and surfactants. In this study, the pure MWCNTs nanopaper and $\text{Fe}_3\text{O}_4/\text{MWCNTs}$ hybrid nanopaper were shown in Figure 1 and their properties can be seen in the Table I.

Hand-layup and resin transfer molding process was used to manufacture laminated composites. One layer of the MWCNT nanopaper (or the $\text{Fe}_3\text{O}_4/\text{MWCNTs}$ hybrid nanopaper) was placed on the bottom of an aluminum mold and then eight plies of GF mats were stacked on the nanopaper (or hybrid

nanopaper) in the same orientation. The resin was then injected into the mold under a pressure of 100 psi at room temperature for overnight, the composite were further post-cure at 120°C for 2 h. The composites samples surface coated MWCNTs buckypaper and $\text{Fe}_3\text{O}_4/\text{MWCNTs}$ hybrid buckypaper were labeled as C_1 and C_2 , respectively.

Characterization

The buckypapers were characterized by X-ray diffraction (XRD) (Rigaku RINT2400 with Cu Ka radiation). Field-emission Scanning electron microscope (FE-SEM) image were taken with a Hitachi S-480 FE-SEM at an acceleration Voltage of 15 kv. Magnetic study was performed by a vibrating sample magnetometer (VSM, Riken Denshi, BHV-525); The dc electrical conductivity measurements were made by the standard four-point contact method on the nanopaper in order to eliminate contact-resistance effects; the complex permittivity ($\epsilon = \epsilon' - j\epsilon''$) and permeability ($\mu = \mu' - j\mu''$) were measured using the waveguide method in the frequency range of 8–18 GHz by Agilent 8720 ET network analyzer. The composite samples of C_1 and C_2 were shown in Figure 1(a,b), whose dimensions were $22.86 \text{ mm} \times 10.16 \text{ mm} \times 2 \text{ mm}$ for X-band and $15.8 \text{ mm} \times 7.9 \text{ mm} \times 2 \text{ mm}$ for Ku-band.

The reflection loss of single-layer composites is calculated by the following equation:

$$\text{RL}(\text{dB}) = 20 \lg \left| \frac{Z_{\text{in}} - Z_0}{Z_{\text{in}} + Z_0} \right| \quad (1)$$

where the input impedance of the absorber Z_{in} is given+

$$Z_{\text{in}} = Z_0 \sqrt{\frac{\mu_r}{\epsilon_r} \tan h \left(j \cdot \frac{2\pi f d}{c} \sqrt{\mu_r \cdot \epsilon_r} \right)} \quad (2)$$

where Z_0 is the impedance of the free space; μ_r and ϵ_r are the relative permeability and permittivity of the absorber; f is the frequency of the electromagnetic wave; d is the thickness of the absorber layer; C is the velocity of light in free space.

RESULTS AND DISCUSSION

Morphology and Element Composition

The morphology and element composition of MWCNTs buckypaper and $\text{Fe}_3\text{O}_4/\text{MWCNTs}$ hybrid buckypaper were investigated by FE-SEM and EDS. There are several distinctive characteristics in the Figure 2(b) compared with a, the MWCNTs in Figure 2(b) have been coated with magnetite nanoparticles whose particle sizes are about 10–30 nm. The distribution of the magnetite nanoparticles on the CNTs surface is quite uniform and no local aggregation is observed. According to the EDS analysis of

Table I. Basic Properties of Buckypaper

	Weight (mg)	Radius (mm)	Thickness (mm)	Conductivity (S/cm)
MWCNTs BP	357.6	50	0.1	26.67
$\text{Fe}_3\text{O}_4/\text{MWCNTs}$ BP	549.2	50	0.105	19.96

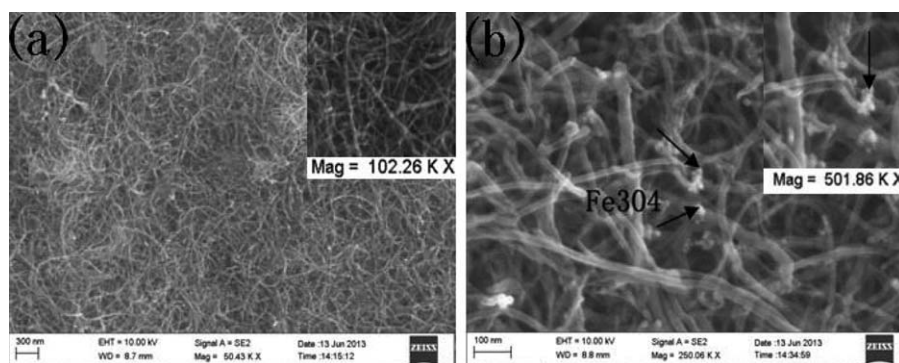


Figure 2. FE-SEM of pure MWCNTs buckypaper (a) and $\text{Fe}_3\text{O}_4/\text{MWCNTs}$ hybrid buckypaper (b).

the Figure 3, it can show that the presence of Fe and O elements in the $\text{Fe}_3\text{O}_4/\text{MWCNTs}$ hybrid buckypaper and the calculated atomic ratio of Fe and O is close to 3 : 4, which further confirmed that the nanoparticles attached on the MWCNTs surface are Fe_3O_4 nanoparticles.

The crystal structure of pure MWCNTs buckypaper and $\text{Fe}_3\text{O}_4/\text{MWCNTs}$ buckypaper are characterized by XRD spectra of Figure 4. The diffraction peaks at $2\theta=26.01^\circ$ and 43.12° are assigned to (0 0 2) and (1 1 0) planes of the graphite structures for MWCNTs. In Figure 4(b), According to the JCPDS file No. 03-0863 for Fe_3O_4 , the other six diffraction peaks (31.68° , 37.03° , 45.18° , 56.39° , 59.70° , and 65.57°) of hybrid buckypapers correspond to the (2 2 0), (3 1 1), (4 0 0), (4 2 2), (5 1 1), (4 4 0) planes of Fe_3O_4 nanoparticles, respectively. The characteristic peaks of MWCNTs remain changed little, which indicates that the graphitic structure of MWCNTs is not obviously decreased during the Fe_3O_4 synthetic treatment.

Electrical Analysis

The conductivities of buckypapers are measured with a RTS-8 digital four probes resistance tester as shown in Table I. It can be seen that the conductivities of $\text{Fe}_3\text{O}_4/\text{MWCNTs}$ buckypaper decrease with addition of Fe_3O_4 particles. Pure MWCNTs buckypaper is a good conductor and its conductivity is 26.7 S/cm. With the addition of Fe_3O_4 particles, MWCNTs can be more tightly wrapped up and the conductivity of $\text{Fe}_3\text{O}_4/\text{MWCNTs}$ buckypaper decreases as shown in Table I. Although the conductivities of $\text{Fe}_3\text{O}_4/\text{MWCNTs}$ buckypapers decrease

with the addition of Fe_3O_4 particle sites, its magnetic property can improve simultaneously. Through tuning up the mass ratio of Fe_3O_4 particle to MWCNTs, the electromagnetic parameters of the hybrid buckypaper can be matched well.

Magnetic Properties of Buckypaper

The hysteresis loop of the $\text{Fe}_3\text{O}_4/\text{MWCNTs}$ hybrid buckypaper is measured at 300 K, Which illustrates the strong magnetic response to a varying magnetic field as shown in Figure 5(b). The saturation magnetization value of $\text{Fe}_3\text{O}_4/\text{MWCNTs}$ hybrid nanopaper is 30.03 emu g^{-1} , which is many times bigger than that of MWCNT buckypaper (0.78 emu g^{-1}) shown in Figure 5(a). The increase of the saturation magnetization can be mainly attributed to the existence of Fe_3O_4 nanoparticles. It is worth mentioning that the $\text{Fe}_3\text{O}_4/\text{MWCNTs}$ hybrid nanopaper has neither coercive force (H_C) nor remanent magnetism (B_r), manifesting its superparamagnetism.¹⁴

Electromagnetic Properties

According to the electromagnetic wave theory, in order to achieve the maximum large absorption, two requirements must be satisfied by microwave-absorbing materials. The first one is the impedance matching performance on the surface of the materials. The second is the EM matching conditions of the materials. In other words, EM parameters must meet the equation $\mu = \epsilon$ in a wide frequency range and the dielectric loss $\tan \delta_\epsilon = \epsilon''/\epsilon'$ and magnetic loss $\tan \delta_\mu = \mu''/\mu'$ are as large as possible. Only in this way can the EM-wave enter the coatings and subsequently be quickly attenuated inside the coatings.

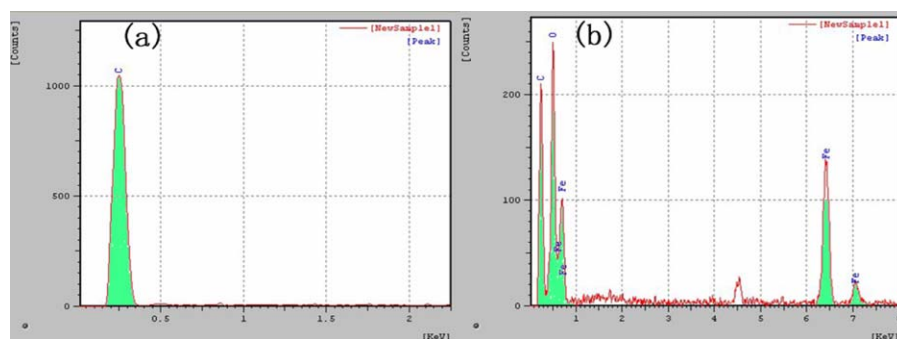


Figure 3. EDS of pure MWCNTs buckypaper (a) and $\text{Fe}_3\text{O}_4/\text{MWCNTs}$ hybrid buckypaper (b). [Color figure can be viewed in the online issue, which is available at wileyonlinelibrary.com.]

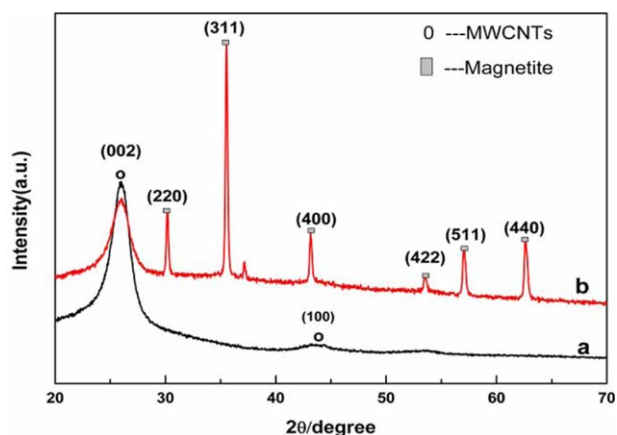


Figure 4. XRD patterns of (a) MWCNTs buckypaper, (b) $\text{Fe}_3\text{O}_4/\text{MWCNT}$ hybrid buckypaper. [Color figure can be viewed in the online issue, which is available at wileyonlinelibrary.com.]

Figure 6 shows the frequency dependence of the real parts ϵ' and the imaginary parts ϵ'' of the complex permittivity for composites C_1 and C_2 in the frequency range of 8–18 GHz. The real part ϵ' of composites C_1 and C_2 show a decrease trend from 6.23 to 0.56 and from 19.02 to 0.48. The imaginary parts ϵ'' of composites C_1 and C_2 show the same decrease trend from 29.50 to 2.59 and from 33.58 to 3.80. The real part of ϵ' and the imaginary parts ϵ'' of composite C_2 are smaller than those of composite C_1 in the frequency range of 9.9–18 GHz as shown in Figure 6. For composite C_2 , the smaller of the real part of ϵ' and the imaginary parts ϵ'' will be very good for improving the absorbing properties. When the electromagnetic wave irradiates on the $\text{Fe}_3\text{O}_4/\text{MWCNTs}$ hybrids, the hybrid capacitance would be generated at the interface of the MWCNTs and Fe_3O_4 nanoparticles and make the dielectric relaxation behavior of the hybrid buckypaper complex, it has also been mentioned in Ref. 15 that the property of interfaces could play a dominant role in determining the dielectric performance. As reported the real part of complex permittivity is an expression

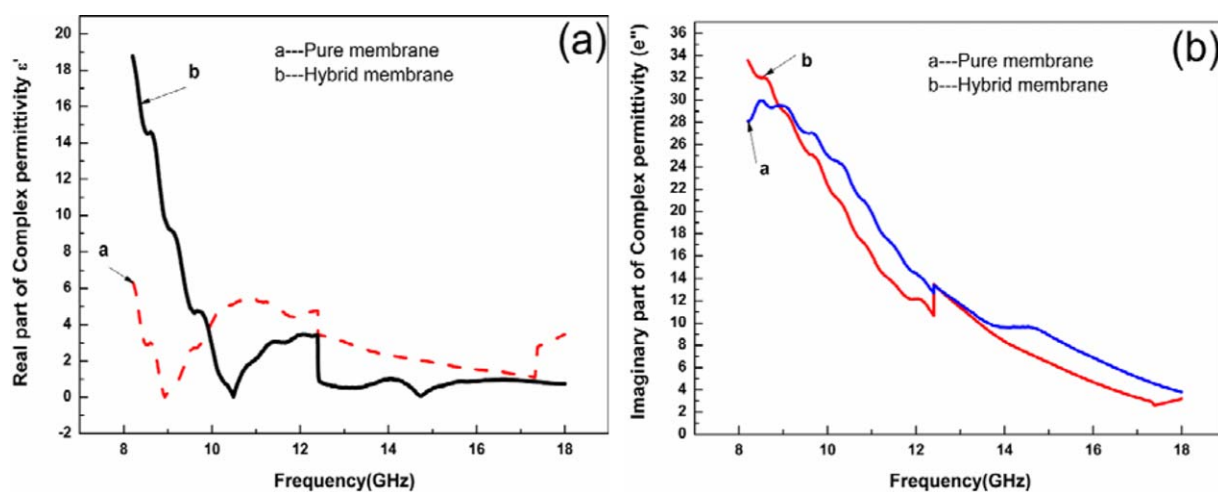


Figure 6. Complex permittivity of C_1 and C_2 . (a) The real part ϵ' , (b) the imaginary parts ϵ'' . [Color figure can be viewed in the online issue, which is available at wileyonlinelibrary.com.]

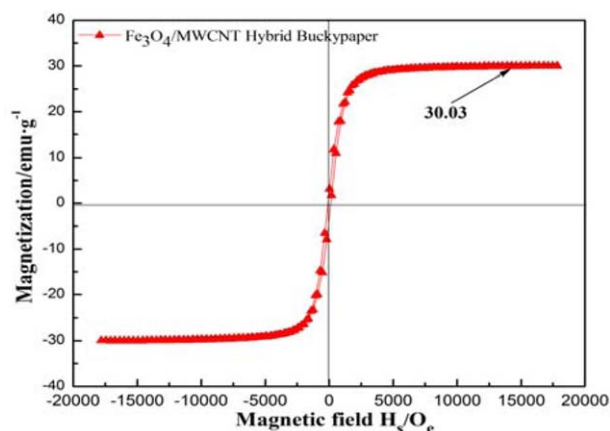
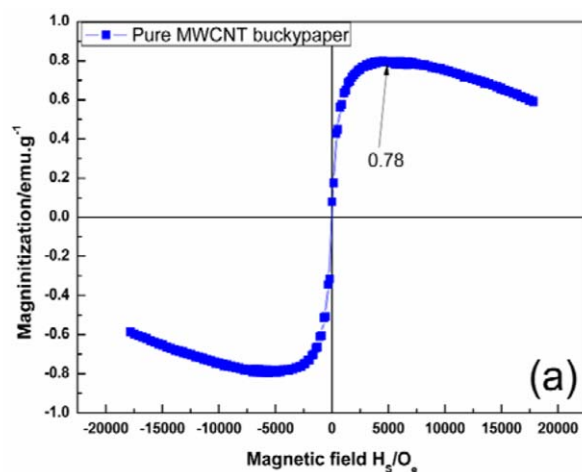


Figure 5. The hysteresis loops of pure MWCNTs buckypaper (a) and $\text{Fe}_3\text{O}_4/\text{MWCNTs}$ hybrid buckypaper (b). [Color figure can be viewed in the online issue, which is available at wileyonlinelibrary.com.]

of polarization capability, the imaginary part is relative to the dielectric loss of a material.¹⁶ It is apparent that the dielectric loss of composite C_2 is mainly caused by interfacial polarization and electric dipolar polarization as Ref. 17 interpreted.

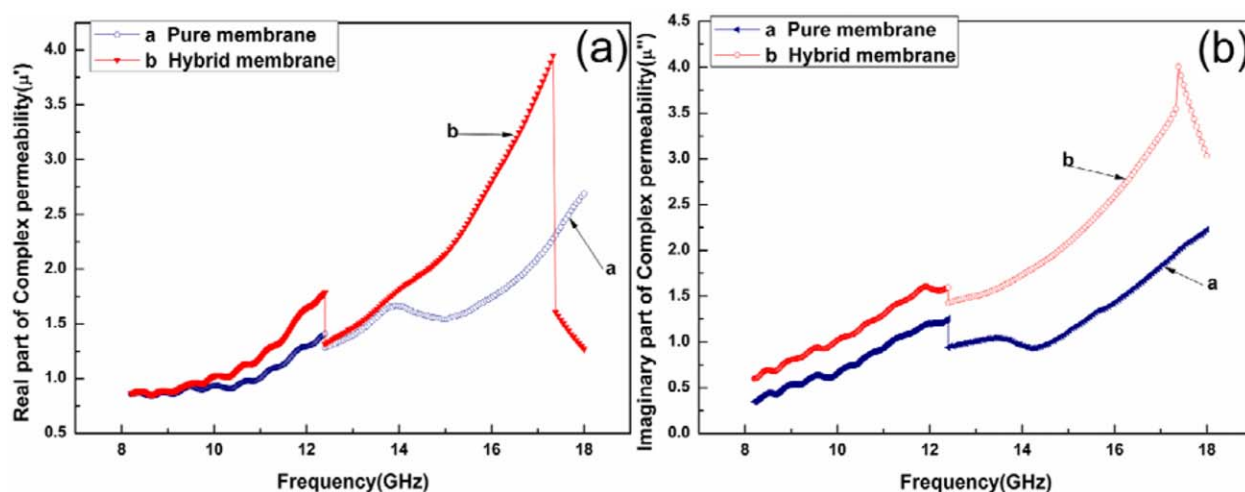


Figure 7. Complex permeability of C_1 and C_2 . (a) The real part μ' , (b) the imaginary parts μ'' . [Color figure can be viewed in the online issue, which is available at wileyonlinelibrary.com.]

Figure 7 shows the frequency dependence of the real parts μ' and imaginary parts μ'' of complex permeability for composites C_1 and C_2 . It exhibits well-proportioned variation and almost same variation tendency in the frequency range of 8–18 GHz, namely, μ' of C_1 and C_2 increase from 0.87 and 0.88 to 2.69 and 3.95. Meanwhile, it is noticed that the μ' value of C_2 is always higher than that of the C_1 , which might due to the core/shell type structure of the $\text{Fe}_3\text{O}_4/\text{MWCNTs}$ hybrids. For imaginary part μ'' , the variation tendencies of the composites C_1 and C_2 are also similar in general. In other words, μ'' of composite C_1 and C_2 present an upgrade tendency from 0.35 and 0.60 to 2.22 and 4.01 in the frequency range of 8–18 GHz. The variation of permeability for composite C_2 can be interpreted as follows: the Fe_3O_4 nanoparticles are magnetic materials, the demagnetizing field generated by the magnetic poles on the surface of the magnetic particles plays a very important role on those permeability.¹⁸ The enhanced permeability will improve the electromagnetic interference absorbing effect by transferring

the electromagnetic energy into heat energy. Generally speaking, the permeability could be explained by hysteresis loss, domain-wall resonance, and natural resonance.¹⁹ The hysteresis loss can be excluded because it appears usually at low frequency region of MHz range. The domain-wall resonance usually takes place at frequency region of 2–5 GHz. For these reasons, natural resonance is deemed to be the main magnetic loss mechanism for the composite sample.

It can be noticed that there are two possible contributions for microwave absorption, namely, dielectric loss ($\tan \delta_e = \epsilon''/\epsilon'$) and magnetic loss ($\tan \delta_\mu = \mu''/\mu'$). In order to understand the actual contribution for the microwave absorption of the composites, both the dielectric loss and magnetic loss of composite C_1 and C_2 were calculated based on the measured complex permeability and permittivity, as shown in Figure 8. The higher magnetic loss of the composites C_2 mainly results from the contribution of both the Fe_3O_4 particles and $\text{Fe}_3\text{O}_4/\text{MWCNTs}/\text{resin}$ three

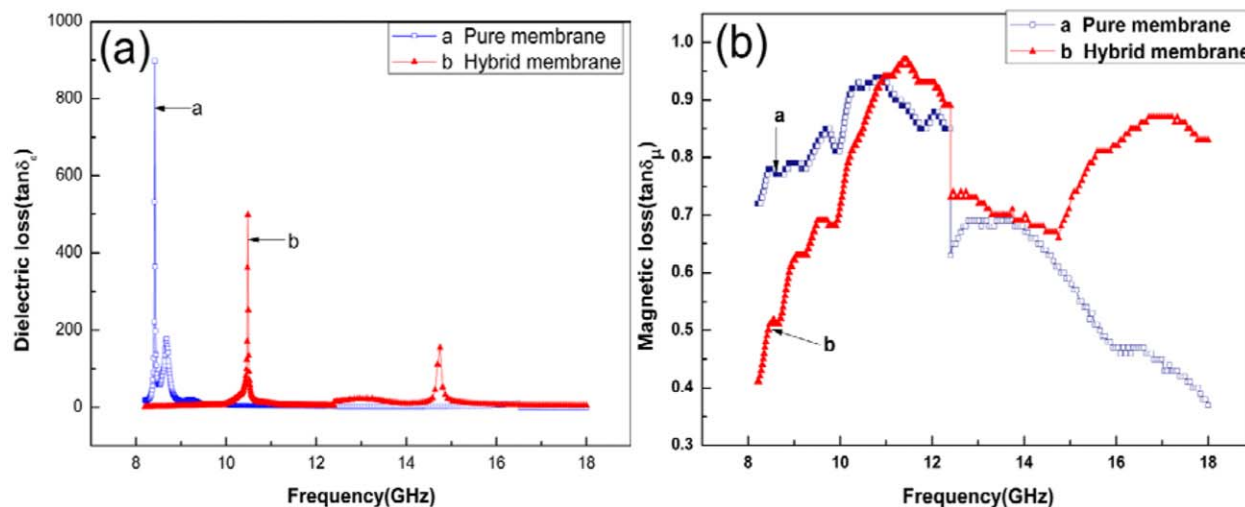


Figure 8. The dielectric loss $\tan \delta_e$ (a) and the magnetic loss $\tan \delta_\mu$ (b) for composites C_1 and C_2 . [Color figure can be viewed in the online issue, which is available at wileyonlinelibrary.com.]

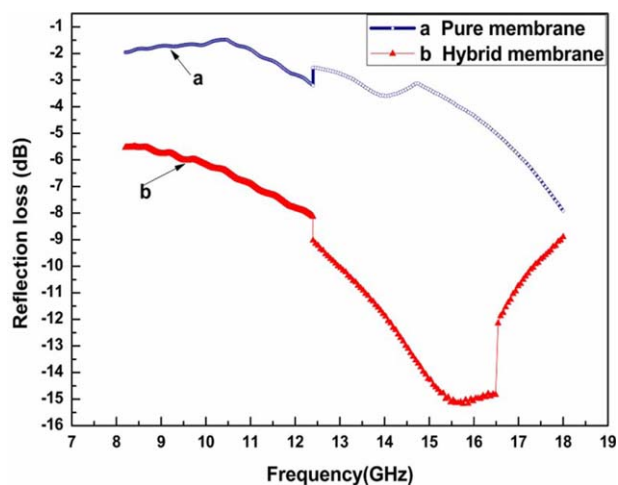


Figure 9. Calculated reflection loss (R_L) versus frequency f of composite C_1 and C_2 . [Color figure can be viewed in the online issue, which is available at wileyonlinelibrary.com.]

dimension complex microstructures. Furthermore, a proper dielectric loss can be obtained by decorated a suitable content of Fe_3O_4 nanoparticles on MWCNTs as shown in Figure 8(a). The magnetic loss changed from 0.37 to 0.94 and 0.41 to 0.97 for C_1 and C_2 in the frequency range of 8–18 GHz. The higher magnetic loss and suitable dielectric loss of composites surface coated $\text{Fe}_3\text{O}_4/\text{MWCNTs}$ hybrid buckypaper can fulfill the impedance matching and attenuation characteristics.

EM-Wave Absorption Performance

According the previous eqs. (1) and (2), the reflection loss is function of six characteristics parameters: ϵ' , ϵ'' , μ' , μ'' , f , d . Thus, if the parameters of the composite are obtained, the absorbing properties of the composites can be calculated by eqs. (1) and (2). Figure 9 shows the frequency dependence of reflection losses for composites C_1 and C_2 with a matching thickness $d = 0.1$ mm. The absorption peak for composite C_2 is -15.3 dB at 15.7 GHz with about 5 GHz bandwidth below -10 dB and 10 GHz bandwidth below -5 dB in the frequency range of 8–18 GHz. The absorption peak for composite C_1 is -7.9 dB at 18 GHz with only about 1.5 GHz bandwidth below -5 dB. In the comparison of Figure 9(a) with Figure 9(b), the reflection loss of C_2 (curve b) is lower than that of C_1 (curve a) in the frequency region of 8–18 GHz. The above results confirmed that $\text{Fe}_3\text{O}_4/\text{MWCNTs}$ hybrid nanopaper could achieve an excellent absorbing ability at X-band and Ku-band with only 0.1 mm matching thickness. In addition, our values are compared to simple mixed method of MWCNTs/CIP²⁰ (-6 dB, 45 wt % CIP, 0.5–1.5 wt % MWCNTs, 0.5 mm), $\text{Fe}_3\text{O}_4/\text{Co}$ ²¹ (-10 dB, 70 wt %, 1.5–2 mm $\text{Fe}_3\text{O}_4/\text{Co}$), and MWCNTs/ Fe_3O_4 hybrid materials²² (-5 dB, 70 wt %, 2 mm). The loading of buckypaper in the total composites structures (0.025 wt %) and the thickness of the hybrid buckypaper (0.1 mm) are far less than above reference, but the microwave-absorbing properties are nearly the same. The $\text{Fe}_3\text{O}_4/\text{MWCNTs}$ hybrid buckypapers can be co-cured with fiber reinforced composites, the loading of the $\text{Fe}_3\text{O}_4/\text{MWCNTs}$ hybrid buckypapers in the absorbing layer exceeds 25% and the Fe_3O_4 nanoparticles were distributed uniformly in

the free-standing porous ways of entangle CNTs. There are more extra interfaces between CNTs and Fe_3O_4 nanoparticles networks in the $\text{Fe}_3\text{O}_4/\text{MWCNTs}$ hybrid buckypapers, the absorbing properties of the hybrid buckypaper was enhanced by the enlargement of the interface area of $\text{Fe}_3\text{O}_4/\text{MWCNTs}$ hybrid buckypapers structures. The $\text{Fe}_3\text{O}_4/\text{MWCNTs}$ hybrid buckypapers fabricated in our work also show relative strong magnetic loss and suitable dielectric loss in the high-frequency range, so the composite surface coated $\text{Fe}_3\text{O}_4/\text{MWCNTs}$ hybrid buckypapers can fulfill the impedance matching characteristic and have wider microwave ability.

CONCLUSION

In this article, $\text{Fe}_3\text{O}_4/\text{MWCNTs}$ hybrids prepared in the presence of PVP were fabricated successfully via *in situ* chemical precipitation method. The $\text{Fe}_3\text{O}_4/\text{MWCNTs}$ hybrids buckypaper made by Vacuum filtration method reveal super paramagnetic and possess a saturation magnetization value of 30.03 emu/g, which is higher than that of pure MWCNTs buckypaper. The maximum reflection loss of composite surface coated $\text{Fe}_3\text{O}_4/\text{MWCNTs}$ hybrid buckypaper with a 0.1 mm matching thickness is -15.3 dB at 15.7 GHz, and the bandwidth below -5 dB is 10 GHz in the frequency range of 8–18 GHz, which is much higher than the composite surface coated pure MWCNTs buckypaper. The unique microwave-absorbing properties of the novel composites structure can be mainly ascribed to the wideband electromagnetic matching, the interfacial electric polarization and the natural resonance. That is to say the $\text{Fe}_3\text{O}_4/\text{MWCNTs}$ hybrids buckypaper can become a promising microwave-absorbing material in the high-frequency range for magnetic applications and absorbing applications.

ACKNOWLEDGMENTS

The authors gratefully acknowledge the financial support by the Defense Industrial Technology Development Program of China (A35201106), Shenyang Science project of China (F11-237-1-100) And Liaoning Province talents support plan of China (LJQ2011018).

REFERENCES

- Iijima, S. *Nature* **1991**, *354*, 56.
- Liu, Z.; Wang, J.; Xie, D. H. *Small* **2008**, *4*, 462.
- Kim, Y. H.; Park, S. J. *Curr. Appl. Phys.* **2011**, *11*, 462.
- Tong, G. X.; Wu, W. H.; Guan, J. G.; Qian, H. S.; Yuan, J. H.; Li, W. J. *Alloy. Compd.* **2011**, *509*, 432026.
- Jiang, F. J.; Pu, H. T.; Yang, Z. L. *New Carbon Mater.* **2007**, *22*, 371.
- Liu, Y.; Jiang, W.; Li, S. *Appl. Surf. Sci.* **2009**, *255*, 7999.
- Wang, X. Z.; Zhao, Z. B.; Qu, J. Y.; Wang, Z. Y.; Qiu, J. S. *J. Phys. Chem. Phys. Solids.* **2010**, *71*, 673.
- Zhou, H.; Zhao, C.; Li, H.; Du, Z. *J. Polym. Sci. Part A. Polym. Chem.* **2010**, *48*, 4697.
- Zhao, C.; Zhang, A.; Zheng, Y.; Luan, J. *Mater. Res. Bull.* **2012**, *47*, 217.

10. Du, C. S.; Pan, N. J. *Power Sources* **2006**, *160*, 1487.
11. Mahajan, S. V.; Hasan, S. A.; Cho, J.; Shaffer, M. S. P.; Boccaccini, A. R.; Dickerson, J. H. *Nanotechnology* **2008**, *19*, 195301.
12. Frackowiak, E.; Khomenko, V.; Jurewicz, K.; Lota, K.; Beguin, F. *Power Sources* **2005**, *153*, 413.
13. Wu, Z.; Chen, Z.; Du, X.; Logan, J. M.; Sippel, J.; Nikolou, M. *Science* **2004**, *305*, 1273.
14. Panczyk, T.; Warzocha, T. P. *Phys. Chem. C* **2009**, *113*, 19155.
15. Tang, X.; Mater, K.-A. *Sci. Eng B* **2007**, *139*, 119.
16. Fang, Z.; Li, C.; Zhang, H.; Zhang, J. *Carbon* **2007**, *45*, 2873.
17. Dakin, T. W. *IEEE* **2006**, *22*, 11.
18. Zhang, B.; Lu, G.; Feng, Y.; Xiong, J. *J. Magn. Magn. Mater.* **2006**, *299*, 205.
19. Xi, L.; Wang, Z.; Zuo, Y.; Shi, X. *Nanotechnology* **2011**, *22*, 045707.
20. Xu, Y. G.; Zhang, D. Y.; Cai, J.; Yuan, I. M.; Zhang, W. Q. *J. Mater. Sci. Tech.* **2012**, *28*, 34.
21. Wang, C.; Chang, Y.; Wang, L.; Liu, C. *Adv. Power Technol.* **2012**.
22. Hou, C. L.; Li, T. H.; Zhao, T. K.; Liu, H. G.; Liu, L. H.; Zhang, W. J. *New carbon Mater.* **2013**, *28*, 184.